

Thermal analysis for peristaltic flow of nanofluid under the influence of porous medium and double diffusion in a non-uniform channel using Sumudu Transformation Method

Asha S. K* and Namrata Kallollikar¹

^{*,1}Department of Mathematics, Karnatak University,

E-mail: as.kotnur2008@gmail.com*

nckallollikar@gmail.com¹

Abstract. The present study aims to investigate the study of double-diffusive convection on peristaltic flow under the assumption of long wavelength and low Reynolds number. The mathematical modelling for a two-dimensional flow, along with double diffusion in nanofluids is considered. The motivation of the present research work is to analyse the effects of thermal radiation on a peristaltic flow through a porous medium in a non-uniform channel. The heat flux of the linear approximation employs the thermal radiation of the flow problem. The governing equations are analytically solved by using Homotopy Perturbation Sumudu Transformation method (HPSTM) with the help of the symbolic software Mathematica. The results of the velocity, pressure rise, temperature, solutal (species) concentration and nanoparticle volume fraction profiles are graphically shown.

Keywords: Peristaltic flow; non-uniform channel; double diffusion; thermal radiation

AMS Mathematics Subject Classification (2010): 76-XX, 76Rxx, 76Sxx, 76Wxx.

1. Introduction

Peristalsis pumping is a unique mechanism and well known to physiologists as a natural mechanism of pumping materials. Peristaltic transport is a form of fluid material transport induced by a progressive wave of area either by contraction or expansion along the length of a distensible tube. This natural phenomenon is known as peristaltic flow. Peristaltic pump is first coined by Latham [1] in 1966 and further research work on Peristaltic flow was extended by Shapiro et al. [2] and Jaffrin et al. [3] many theoretical and experimental studies have been discussed for the various type of fluid flow channel in Peristalsis motion. Peristaltic flow occurs widely in various physiological functions such as blood flow in small vessels of the human circulator system, semen transport in vas deferens, movement of ovum in the fallopian tube, bile transport from gall bladder to duodenum, ingesting food via the esophagus, chyme movement in the gastrointestinal tract, vasomotion of blood vessels such as veins, capillaries and vertebral arteries, transport of urine from the kidney to the bladder, transport of hygienic fluids, transfer of corrosive fluids, transport of toxic fluids in the nuclear power industry.

Phenomenon of Peristaltic transport in non-uniform ducts may be of considerable interest, it is noted that many physiological problems are known to be of non-uniform cross-section. Gupta et al [4] and Srivastava et al [5] have considered peristaltic transport in non-uniform channels. It is seen in many physiological structures that the ducts are either in uniform or non-uniform cross section. It is well known that the human body is made up of several non-uniform ducts, for example lymphatic vessels, intestine, ducts efferent's of the reproductive tract. Some other works are done on theoretical studies of peristaltic transport of physiological fluids in vessels of non-uniform cross section [6-8].

Double diffusion is the phenomenon in which mass and heat transfers occur concurrently with complicity of the fluid motion. Research on peristaltic flow of double-diffusive convection is an innovative concept. Double diffusion has important applications in chemical engineering, geophysics, oceanography, solid-state physics, astrophysics and also many engineering applications like natural gas storage tanks, solar ponds, metal solidification processes and crystal manufacturing. Peristaltic pumping with double diffusive convection in nanofluid was studied by [9-12]. They show double diffusive effect with other nanofluid models.

Effects of thermal radiation and heat generation/absorption on hydromagnetic peristaltic flow is of considerable significance for many scientific and engineering applications viz. heating and freezing of chambers, fossil fuel combustion energy processes, evaporation from massive open water reservoirs, propulsion devices for aircraft, missiles, satellites and space vehicles etc. The research work on peristaltic motion with the influence of thermal radiation is reported in References [13-15]. They show the effect of some other physical parameter like Hartmann number, thermophoresis and Brownian parameters.

In all abovementioned investigations reveal that the role of thermal radiation effects on double diffusive convection of nanofluid in non-uniform cross-section has not yet been studied in literature. The motivation of the present research work is to analyse the effects of thermal radiation on a peristaltic flow through a porous medium in a non-uniform channel. Double diffusive convection problems have so many practical applications in oceanography, geophysics, biology, and astrophysics. Heat transfer rate is controlling by applying the radiation. The basic governing equations are highly nonlinear, which are solved by using Homotopy perturbation Sumudu transformation method (HPSTM) [16-20] and analysis of the embedded parameters on velocity, pressure rise, energy, solutal (species) concentration, and nanoparticle volume fraction is shown in the form of graphs.

2. Mathematical analysis

Here we have considered the two-dimensional peristaltic flow of non-uniform channel with the sinusoidal waves of small amplitudes propagates the speed of the channel walls. c is the constant speed of the channel (Figure 1).

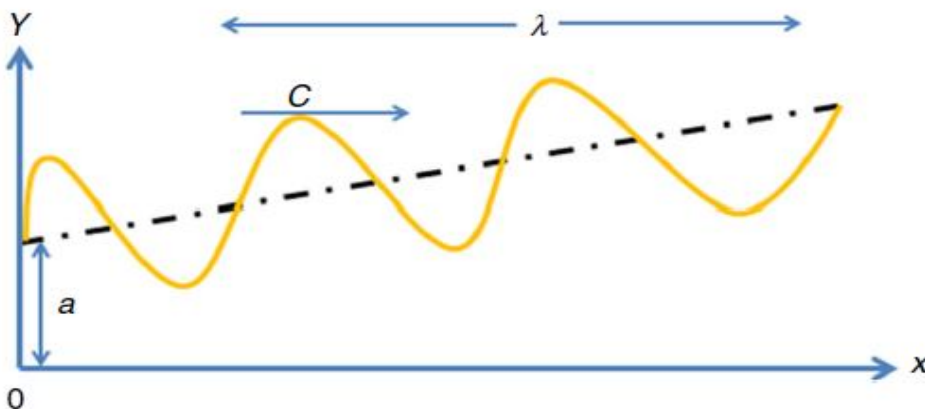


Fig. 1 Geometry of a peristaltic transport through a non-uniform channel

The geometric model of the channel is defined as

$$h'(X,t) = a + d \sin \left[\frac{2\pi}{\lambda} (\bar{X} - c\bar{t}) \right] \quad (1)$$

Where $a = a_0 + k\bar{X}$ is the channel half width, c is the constant wave speed, λ is the wavelength, \bar{t} is the time and d represents the amplitude of the wave. The velocity components \bar{U} and \bar{V} along the \bar{X} and \bar{Y} directions respectively, in the fixed frame, the velocity field V is taken as

$$V = [\bar{U}(\bar{X}, \bar{Y}, \bar{t}), \bar{V}(\bar{X}, \bar{Y}, \bar{t}), 0] \quad (2)$$

The radiative heat flux q_r can be written as

$$q_r = -16 \frac{\sigma^* T_1'^3}{3k^*} \frac{\partial T'}{\partial y'} \quad (3)$$

In the above equation, k^* is the Rosseland mean absorption coefficient and σ^* denotes the Stefan-Boltzmann constant. Considering the nanofluid flow temperature is very small, therefore the term is a linear function of temperature.

The basic governing equations describing the peristaltic flow patterns for the nanofluid are as follows:

$$\frac{\partial U'}{\partial x'} + \frac{\partial V'}{\partial y'} = 0, \quad (4)$$

$$\rho f \left(\frac{\partial U'}{\partial t'} + U' \frac{\partial U'}{\partial x'} + V' \frac{\partial U'}{\partial y'} \right) = -\frac{\partial p'}{\partial x'} + \mu \left(\frac{\partial^2 U'}{\partial x_2'^2} + \frac{\partial^2 U'}{\partial y_2'^2} \right) + \rho f g (\varphi' - \varphi_0') \quad (5)$$

$$+ \rho f g (T' - T_0') - g(\rho_p - \rho f_0)(F' - F_0'),$$

$$\rho f \left(\frac{\partial V'}{\partial t'} + U' \frac{\partial V'}{\partial x'} + V' \frac{\partial V'}{\partial y'} \right) = -\frac{\partial p'}{\partial y'} + \mu \left(\frac{\partial^2 V'}{\partial x_2'^2} + \frac{\partial^2 V'}{\partial y_2'^2} \right),$$

(6)

$$(\rho c)_f \left(\frac{\partial T'}{\partial t'} + U' \frac{\partial T'}{\partial x'} + V' \frac{\partial T'}{\partial y'} \right) = k_T \left(\frac{\partial^2 T'}{\partial x_2'^2} + \frac{\partial^2 T'}{\partial y_2'^2} \right) + \frac{D_{TC} \alpha C_p}{C_s} \left(\frac{\partial^2 \varphi'}{\partial x_2'^2} + \frac{\partial^2 \varphi'}{\partial y_2'^2} \right) - \frac{\partial^2 q_r}{\partial y_2'^2}$$

$$+ (\rho c)_p D_B \left(\frac{\partial F'}{\partial x'} \frac{\partial T'}{\partial x'} + \frac{\partial F'}{\partial y'} \frac{\partial T'}{\partial y'} \right) + (\rho c)_p \frac{D_T}{T_m} \left[\left(\frac{\partial T'}{\partial x'} \right)^2 + \left(\frac{\partial T'}{\partial y'} \right)^2 \right],$$

(7)

$$\frac{\partial \varphi'}{\partial t'} + U' \frac{\partial \varphi'}{\partial x'} + V' \frac{\partial \varphi'}{\partial y'} = D_{CT} \left(\frac{\partial^2 \varphi'}{\partial x_2'^2} + \frac{\partial^2 \varphi'}{\partial y_2'^2} \right) + D_s \left(\frac{\partial^2 T'}{\partial x_2'^2} + \frac{\partial^2 T'}{\partial y_2'^2} \right),$$

(8)

$$\frac{\partial F'}{\partial t'} + U' \frac{\partial F'}{\partial x'} + V' \frac{\partial F'}{\partial y'} = D_B \left(\frac{\partial^2 F'}{\partial x_2'^2} + \frac{\partial^2 F'}{\partial y_2'^2} \right) + \frac{D_T}{T_m} \left(\frac{\partial^2 T'}{\partial x_2'^2} + \frac{\partial^2 T'}{\partial y_2'^2} \right),$$

(9)

where $(\rho c)_f$ is the heat capacity of the fluid, D_{TC} is the Dufour diffusivity, k_T is the thermal conductivity of the fluid, $(\rho c)_p$ is the effective heat capacity of the nanoparticle material, g is the gravity, φ' is the solutal

(species) concentration, K_0 is permeability constant of the porous medium, and σ is electrically conductivity of the fluid. Furthermore, ρ_f is the effective density, D_T is thermophoresis diffusion coefficient, D_s is the solutal diffusivity, C_p is the specific heat at constant pressure, α is the thermal diffusion ratio, C_s is the concentration susceptibility, D_{CT} is the Soret diffusivity, and T_m is the mean fluid temperature.

The connection between the wave frame and laboratory frame are introduced through

$$u' = U' - c, \quad y' = y', \quad v' = V', \quad x' = x' - ct'. \quad (10)$$

Introducing the following nondimensional variables

$$\left. \begin{aligned} \psi &= \frac{\psi'}{ca_o}, \quad x = \frac{x'}{\lambda}, \quad y = \frac{y'}{a_o}, \quad t = \frac{ct'}{\lambda}, \quad v = \frac{v'}{c}, \quad \delta = \frac{a_o}{\lambda}, \quad p = \frac{p'a_o^2}{\mu c \lambda} \\ u &= \frac{u'}{c}, \quad \alpha = \frac{k_T}{(\rho c)_f}, \quad Pr = \frac{\mu}{\alpha}, \quad b = \frac{d}{a_o}, \quad N_{TC} = \frac{D_{TC} \alpha C_p (\phi'_1 - \phi'_0)}{\mu k_T C_s (T'_1 - T'_0)} \\ \theta &= \frac{T' - T'_0}{T'_1 - T'_0}, \quad \varphi = \frac{\phi' - \phi'_0}{\phi'_1 - \phi'_0}, \quad \gamma = \frac{F' - F'_0}{F'_1 - F'_0}, \quad Nt = \frac{(\rho c)_p D_T (T'_1 - T'_0)}{(\rho c)_f \mu T_m} \\ Rd &= 16 \frac{\sigma^* T_1'^3}{3k^* k_T}, \quad h = \frac{h'}{a_o}, \quad f^* = \frac{q}{ca_o}, \quad Gr_t = \frac{\rho_f g a_o^2 (T'_1 - T'_0)}{c \mu} \\ Gr_c &= \frac{\rho_f g a_o^2 (\phi'_1 - \phi'_0)}{c \mu}, \quad N_{TC} = \frac{D_{CT} (T'_1 - T'_0)}{D_s (\phi'_1 - \phi'_0)}, \quad Re = \frac{\rho_f c a_o}{\mu} \\ Gr_F &= \frac{(\rho_p - \rho_{f_0}) g a_o^2 (F'_1 - F'_0)}{c \mu}, \quad Nb = \frac{(\rho c)_p D_B (F'_1 - F'_0)}{(\rho c)_f \mu}. \end{aligned} \right\} \quad (11)$$

where δ is the dimensionless wave number, θ is the dimensionless temperature, φ is the nanoparticle volume

fraction, and the stream function taken as $v = -\delta \frac{\partial \psi}{\partial X}$ and $u = \frac{\partial \psi}{\partial y}$.

By using Equation (11), Equations (4) to (10) can be written as

$$\frac{\partial p}{\partial x} = \frac{\partial^2 u}{\partial y^2} + Gr_T \theta + Gr_c \varphi - Gr_F \gamma, \quad (12)$$

$$\frac{\partial p}{\partial y} = 0, \quad (13)$$

$$\frac{\partial^3 \psi}{\partial y^3} + Gr_T \frac{\partial \theta}{\partial y} + Gr_c \frac{\partial \varphi}{\partial y} - Gr_F \frac{\partial \gamma}{\partial y} = 0, \quad (14)$$

$$\frac{\partial^2 \theta}{\partial y^2} + Nb \text{Pr} \frac{\partial \theta}{\partial y} \frac{\partial \gamma}{\partial y} + N_{rc} \text{Pr} \frac{\partial^2 \varphi}{\partial y^2} + Nt \text{Pr} \left(\frac{\partial \theta}{\partial y} \right)^2 + Rd \frac{\partial^2 \theta}{\partial y^2} = 0,$$

(15)

$$\frac{\partial^2 \varphi}{\partial y^2} + N_{ct} \frac{\partial^2 \theta}{\partial y^2} = 0,$$

(16)

$$\frac{\partial^2 \gamma}{\partial y^2} + \frac{Nt}{Nb} \frac{\partial^2 \theta}{\partial y^2} = 0.$$

(17)

The corresponding dimensionless boundary conditions can be written in the following form

$$\left. \begin{aligned} \psi=0, \quad \frac{\partial^2 \psi}{\partial y^2}=0, \quad \theta=0, \quad \gamma=0 \quad \text{at} \quad y=0, \\ \psi=f^*, \quad \frac{\partial \psi}{\partial y}=-1, \quad \theta=1, \quad \gamma=0 \quad \text{at} \quad y=h=1+\frac{\lambda k_o x}{a_o}+b \sin[2\pi(x-t)]. \end{aligned} \right\}$$

(18)

where f^* is the wave frame it is related to the dimensionless time mean flow rate Θ in the laboratory frame as follows

$$\Theta = f^* + 1, \quad f^* = \int_0^h \frac{\partial \psi}{\partial y} dy,$$

(19)

where $\Theta = \frac{Q}{sa_1}$ and $f^* = \frac{q}{sa_1}$ are the dimensionless time mean flow rate in a fixed and wave frames respectively.

The coupled partial differential Equations (14) to (19) with the boundary conditions (18) are solved by using Homotopy perturbation sumudutransformtion method (HPSTM) and the analysis of the present method of solution is mentioned in the below section.

3. Method of solution

The governing equations (12) to (17) are evaluated by HPSTM. This method is an analytical technique, which can be used to calculate the nonlinear problems that contains large and small physical parameters(solution is obtained in terms of convergent series solutions).

In this section, we apply the HPSTM to the governing equations to obtain an approximate analytical solution. By applying the sumudu transform, inverse sumudu transform on both sides of the governing equations we get,

$$u(y) = ay + y \frac{\partial p}{\partial x} - s^{-1} \left[v^2 s \left[Gr_T \theta - Gr_C \varphi + Gr_F \gamma \right] \right], \quad (20)$$

$$\psi(y) = ay^2 - s^{-1} \left[u^3 s \left[Gr_T \frac{\partial \theta}{\partial y} + Gr_C \frac{\partial \varphi}{\partial y} + Gr_F \frac{\partial \gamma}{\partial y} \right] \right], \quad (21)$$

$$\theta(y) = ay - s^{-1} \left[u^2 s \left[\frac{Nb \text{Pr}}{1+Rd} \frac{\partial \theta}{\partial y} \frac{\partial \gamma}{\partial y} + \frac{N_{TC} \text{Pr}}{1+Rd} \frac{\partial^2 \varphi}{\partial y^2} + \frac{Nt \text{Pr}}{1+Rd} \left(\frac{\partial \theta}{\partial y} \right)^2 \right] \right],$$

(22)

$$\varphi(y) = ay - s^{-1} \left[u^2 s \left[N_{CT} \frac{\partial^2 \theta}{\partial y^2} \right] \right],$$

(23)

$$\gamma(y) = ay - s^{-1} \left[u^2 s \left[\frac{Nt}{Nb} \frac{\partial^2 \theta}{\partial y^2} \right] \right].$$

(24)

Now applying HPM,

$$\sum_{m=0}^{\infty} p^m u_m = ay + y \frac{\partial p}{\partial x} - s^{-1} \left[v^2 s \left[Gr_T \sum_{m=0}^{\infty} p^m H_{1_m} - Gr_C \sum_{m=0}^{\infty} p^m M_{1_m} + Gr_F \sum_{m=0}^{\infty} p^m C_{1_m} \right] \right],$$

(25)

$$\sum_{m=0}^{\infty} p^m \theta_m(y) = ay - s^{-1} \left[u^2 s \left[\frac{Nb Pr}{1+Rd} \sum_{m=0}^{\infty} p^m H_{2_m}(y) + \frac{Nt Pr}{1+Rd} \sum_{m=0}^{\infty} p^m M_{2_m}(y) + \frac{Nt Pr}{1+Rd} \sum_{m=0}^{\infty} p^m \left((\theta_m)_y \right)^2 \right] \right], \quad (26)$$

$$\sum_{m=0}^{\infty} p^m \gamma(y) = ay - s^{-1} \left[u^2 s \left[\frac{Nt}{Nb} \sum_{m=0}^{\infty} p^m H_{3_m} \right] \right], \quad (27)$$

$$\sum_{m=0}^{\infty} p^m \varphi(y) = ay - s^{-1} \left[u^2 s \left[N_{CT} \sum_{m=0}^{\infty} p^m H_{4_m} \right] \right],$$

(28)

$$\sum_{m=0}^{\infty} p^m \psi_m(y) = ay^2 - s^{-1} \left[u^3 s \left[Gr_T \sum_{m=0}^{\infty} p^m H_{5_m}(y) + Gr_C \sum_{m=0}^{\infty} p^m M_{5_m}(y) + Gr_F \sum_{m=0}^{\infty} p^m C_{5_m} \right] \right],$$

(29)

where , $H_{1_m}, M_{1_m}, C_{1_m}, H_{2_m}, M_{2_m}, H_{3_m}, H_{4_m}, H_{5_m}, M_{5_m}, C_{5_m}$ are He's polynomials. So He's polynomials are given by

$$H_m(U_0, U_1, U_2, \dots, U_m) = \frac{1}{m!} \frac{\partial^m}{\partial p^m} \left[N \left(\sum_{i=0}^{\infty} p^i U_i \right) \right]_{p=0}. \quad (30)$$

Comparing the coefficient of like powers of p in equation 25 to 29, we get the required approximations and we get the solution as follows

$$u = ay + y \frac{\partial p}{\partial x} - Gr_T a \frac{y^3}{6} - Gr_C a \frac{y^3}{6} + Gr_F a \frac{y^3}{6} + Gr_F \frac{y^3}{6} + \frac{Nb Pr}{1+Rd} Gr_T a^2 \frac{y^4}{96} + \frac{Nt Pr}{1+Rd} Gr_T a^2 \frac{y^4}{96} + \dots$$

(31)

$$\theta = ay - \frac{Nb Pr}{1+Rd} a^2 \frac{y^2}{2} - \frac{Nt Pr}{1+Rd} a^2 \frac{y^2}{2} + \frac{Nb^2 Pr^2}{(1+Rd)^2} a^3 \frac{y^3}{6} + \frac{Nb Nt Pr^2}{(1+Rd)^2} a^3 \frac{y^3}{6} - \frac{Nt Pr}{1+Rd} \left(-\frac{Nb Pr}{1+Rd} a^2 - \frac{Nt Pr}{1+Rd} a^2 \right)^2 \frac{y^2}{2} + \dots$$

(32)

$$\gamma = ay + \frac{Nt \Pr}{1+Rd} a^2 \frac{y^2}{2} + \frac{Nt^2 \Pr}{Nb(1+Rd)} a^2 \frac{y^2}{2} - \frac{NbNt \Pr^2}{(1+Rd)^2} a^3 \frac{y^3}{6} - \frac{Nt^2 \Pr^2}{(1+Rd)^2} a^3 \frac{y^3}{6} + \frac{Nt^2 \Pr}{Nb(1+Rd)} \left(-\frac{Nb \Pr}{1+Rd} a^2 - \frac{Nt \Pr}{1+Rd} a^2 \right)^2 \frac{y^2}{2} + \dots \quad (33)$$

$$\varphi = ay + \frac{N_{CT} Nb \Pr}{1+Rd} a^2 \frac{y^2}{2} + \frac{N_{CT} Nt \Pr}{1+Rd} a^2 \frac{y^2}{2} - \frac{N_{CT} Nb^2 \Pr^2}{(1+Rd)^2} a^3 \frac{y^3}{6} - \frac{N_{CT} Nb Nt \Pr^2}{(1+Rd)^2} a^3 \frac{y^3}{6} + \frac{N_{CT} Nt \Pr}{(1+Rd)} \left(-\frac{Nb \Pr}{1+Rd} a^2 - \frac{Nt \Pr}{1+Rd} a^2 \right)^2 \frac{y^2}{2} + \dots \quad (34)$$

$$\psi = ay^2 - Gr_T a \frac{y^3}{6} - Gr_C a \frac{y^3}{6} + Gr_F a \frac{y^3}{6} + Gr_T \frac{Nb \Pr}{1+Rd} a^2 \frac{y^4}{24} + Gr_T \frac{Nt \Pr}{1+Rd} a^2 \frac{y^4}{24} + \dots \quad (35)$$

The volume flow rate is given by

$$Q = \int_0^h u dy. \quad (36)$$

Integrating equation (36) and after manipulating we get,

$$\frac{\partial p}{\partial x} = 2Q - a + Gr_T a \frac{1}{9} + Gr_C a \frac{1}{9} - Gr_F a \frac{1}{9} - \frac{Nb \Pr}{1+Rd} Gr_T a^2 \frac{1}{192} - \frac{Nt \Pr}{1+Rd} Gr_T a^2 \frac{1}{192}. \quad (37)$$

The volume flow rate in fixed frame is given by

$$Q = \int_0^h (u+1) dy, \quad (38)$$

$$Q = q + h. \quad (39)$$

Averaging volume flow rate

$$\bar{Q} = \int_0^1 Q dt = \int_0^1 (q+h) dt. \quad (40)$$

This implies

$$\bar{Q} = q + 1 = 1 + Q - h. \quad (41)$$

From equation (37) and (41) the pressure gradient is expressed in terms of averaged flow rate as

$$\frac{\partial p}{\partial x} = 2(\bar{Q} - 1 + h) - a + Gr_T a \frac{1}{9} + Gr_C a \frac{1}{9} - Gr_F a \frac{1}{9} - \frac{Nb \Pr}{1+Rd} Gr_T a^2 \frac{1}{192} - \frac{Nt \Pr}{1+Rd} Gr_T a^2 \frac{1}{192}. \quad (42)$$

The pressure rise across one wavelength (Δp) is computed using

$$\Delta p = \int_0^1 \frac{\partial p}{\partial x} dx. \quad (43)$$

We get,

$$\Delta p = 2(\bar{Q} - 1 + h) - a + Gr_T a \frac{1}{9} + Gr_C a \frac{1}{9} - Gr_F a \frac{1}{9} - \frac{Nb Pr}{1 + Rd} Gr_T a^2 \frac{1}{192} - \frac{Nt Pr}{1 + Rd} Gr_T a^2 \frac{1}{192}. \quad (44)$$

4. Discussion

Using HPSTM we have solved the nonlinear partial differential equations. We have used symbolic software Mathematica in the present work. Through the codes of the software Mathematica we have obtained the solutions of HPSTM for velocity, pressure rise, temperature, volume fraction of nanoparticles and solutal (species) concentration profiles and graphical results are plotted in Origin Software. This section constitutes the analysis of different values of physical parameters on velocity, pressure rise, temperature, solutal concentration, and nanoparticle volume fraction.

4.1 Velocity distribution

The effects of thermal Grashof number Gr_T , solutal Grashof number Gr_C , and nanoparticle Grashof number Gr_F on velocity profile are representing through the Figures 2 to 4. Opposite behaviour can be observed in both Gr_T and Gr_C . The opposite behaviour can be seen in the case of solutal Grashof number Gr_C . As thermal Grashof number Gr_T satisfies the relative influence of thermal buoyancy force and viscous hydrodynamic force. Due to which increasing the thermal Grashof number Gr_T the magnitude of the velocity decreases, For higher values of solutal Grashof number Gr_C the velocity profile increases. Figure 4 shows the effect of nanoparticle Grashof number Gr_F on velocity profile. It is observed that the velocity profile decreases with increasing the Gr_F .

4.2 Pressure rise

Figures 5-7 are plotted to the different physical parameters they are thermal Grashof number Gr_T , Solutal Grashof number Gr_C and nanoparticle Grashof number Gr_F on pressure rise Δp against flow rate Q . We observed that Figure 5 shows the pressure rise for different values of nanoparticle thermal Grashof number Gr_T . We noticed that the pressure rise increases with a higher value of Grashof number Gr_T . Figures 6 and 7 shows the pressure rise for different values of nanoparticle thermal solute Grashof number Gr_C and Grashof number Gr_F . the pressure rise decreases with an increase in solutal Grashof number Gr_C and nanoparticle Grashof number Gr_F . Physically, it is valid because concentration of nanoparticles in the fluid increases, which cause decreasing the pressure.

4.3 Temperature distribution

Figures 8-10 depicted for different values of Brownian motion parameter Nb , thermophoresis parameter and the thermal radiation parameter Rd . From Figures 13 and 14, it is observed that there is enhancement in temperature profile for different values of Brownian motion parameter Nb and thermophoresis parameter Nt . The increase of Brownian motion parameter Nb cause the random motion of fluid particles that produce more heat, so there is temperature rises in the system, which can be seen in Figure 8, whereas, in Figure 9, the temperature profile increases as the fluid particles are moved away from the cold surface to hot surface by increasing the thermophoresis parameter Nt . In Figure 10, the opposite behaviour can be seen, that is, the decay in the temperature profile with an increase of thermal radiation Rd . It is due to fact that the thermal radiation is inversely proportional with thermal conduction parameter K_T , therefore maximum heat is radiated away from the system, which leads to reduction in the heat conduction of the fluid.

4.4 Solutal (species) concentration distribution

The solutal (species) concentration profile is examined by the profile of Nb , Nt , N_{CT} . Effects Nb and Nt are discussed using Figures 11 and 12. From these two figures, we can observe that the solutal (species) concentration profile has the similar behaviour on both Nb and Nt , and solutal (species) concentration decreases with an increasing of N_{CT} we can observe this in figure 13.

4.5 Nanoparticle volume fraction distribution

The nanoparticle concentration visualizations for the influences of Nb , Nt on peristaltic flow in the presence of nanofluids has been shown in figures 14 and 15. The nanoparticle volume fraction of fluid increases with increase in Brownian motion parameter Nb . Because in the case of nanofluids temperature distribution is large, which can lead to the distribution of the system which is shown in figure 14. However, the opposite behaviour is seen in the case of thermophoresis parameter figure 15.

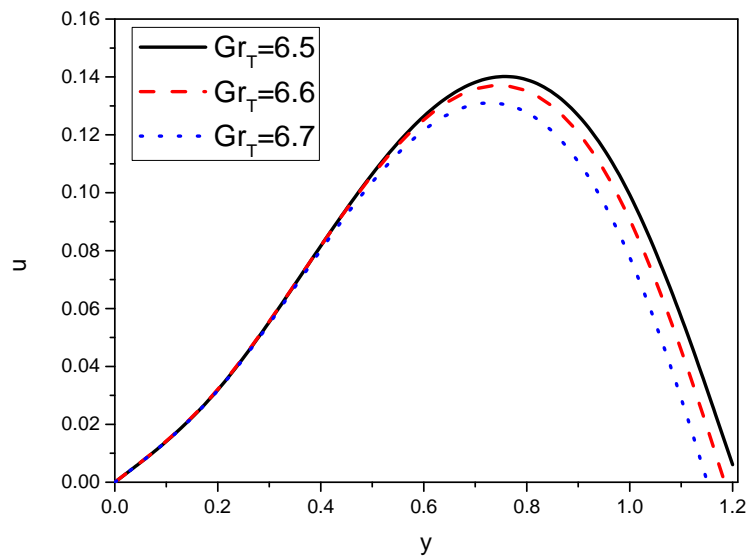


FIGURE 2 Velocity profile for different values of Gr_T
When $Gr_C = 6.5$, $Gr_F = 6.5$, $Nt = 0.5$, $Nb = 0.5$, $Pr = 1$, $Rd = 0.1$

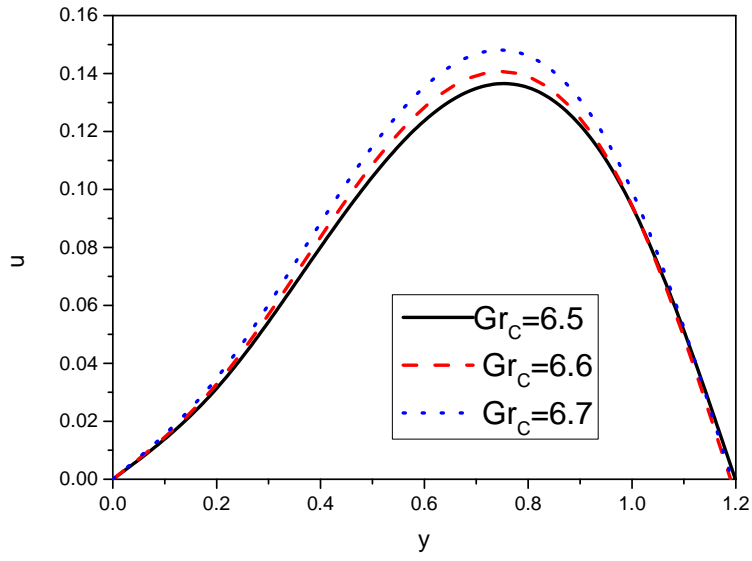


FIGURE 3 Velocity profile for different values of Gr_C
 $Gr_T=6.5$, $Gr_F=6.5$, $Nt=0.5$, $Nb=0.5$, $Pr=1$, $Rd=0.1$

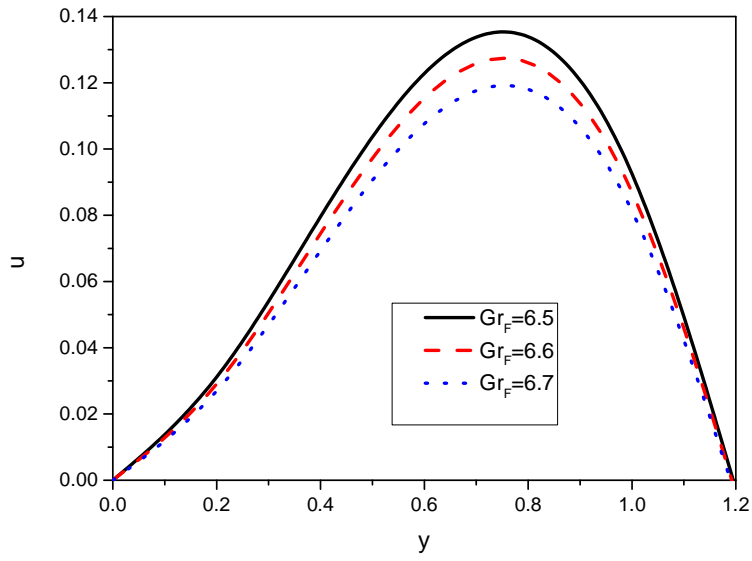


FIGURE 4 Velocity profile for different values of Gr_F
 $Gr_T=6.5$, $Gr_C=6.5$, $Nt=0.5$, $Nb=0.5$, $Pr=1$, $Rd=0.1$

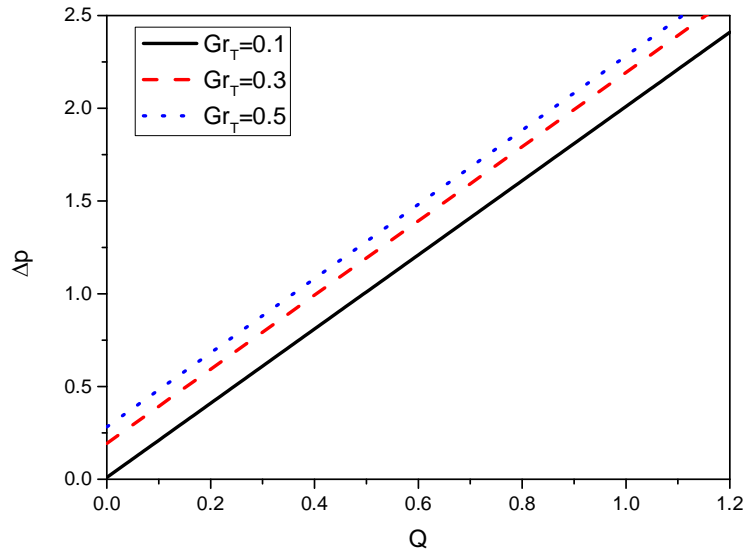


FIGURE 5 Pressure rise for various values of Gr_T
when $Gr_C = 0.8$, $Gr_F = 0.8$, $Nt = 0.6$, $Nb = 0.6$, $Pr = 7.0$, $Rd = 0.5$

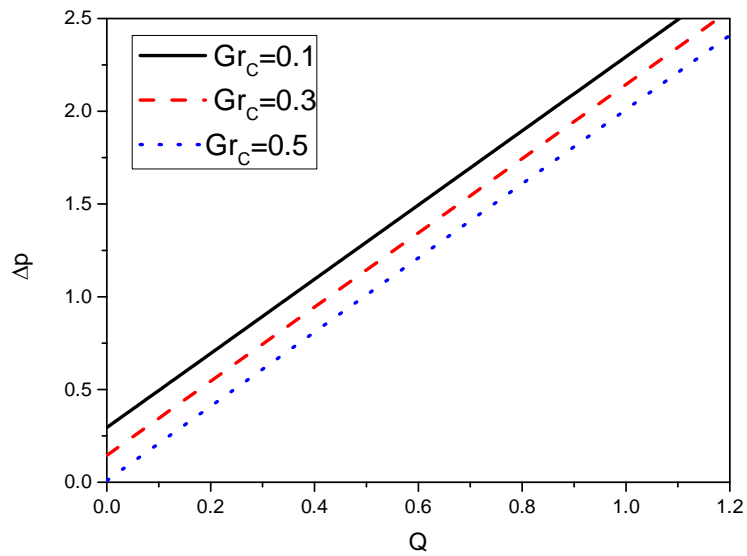


FIGURE 6 Pressure rise for various values of Gr_C
when $Gr_T = 0.8$, $Gr_F = 0.8$, $Nt = 0.6$, $Nb = 0.6$, $Pr = 7.0$, $Rd = 0.5$

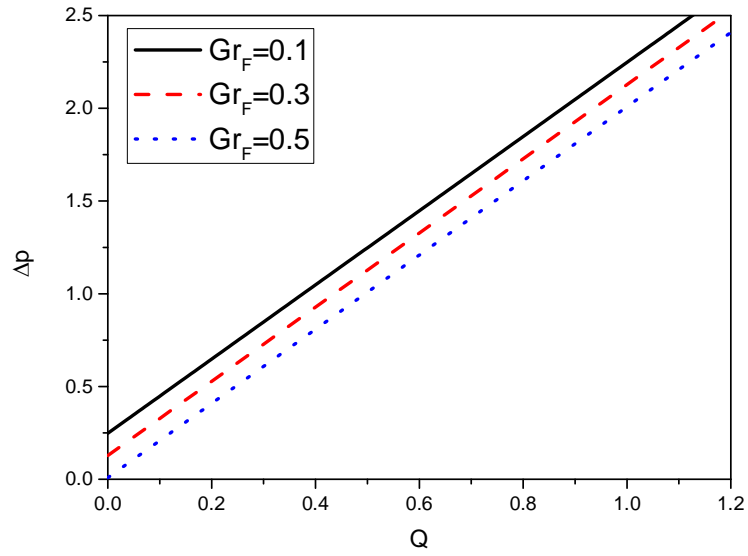


FIGURE 7 Pressure rise for various values of Gr_F
 when $Gr_T = 0.8$, $Gr_C = 0.8$, $Nt = 0.6$, $Nb = 0.6$, $Pr = 7.0$, $Rd = 0.5$

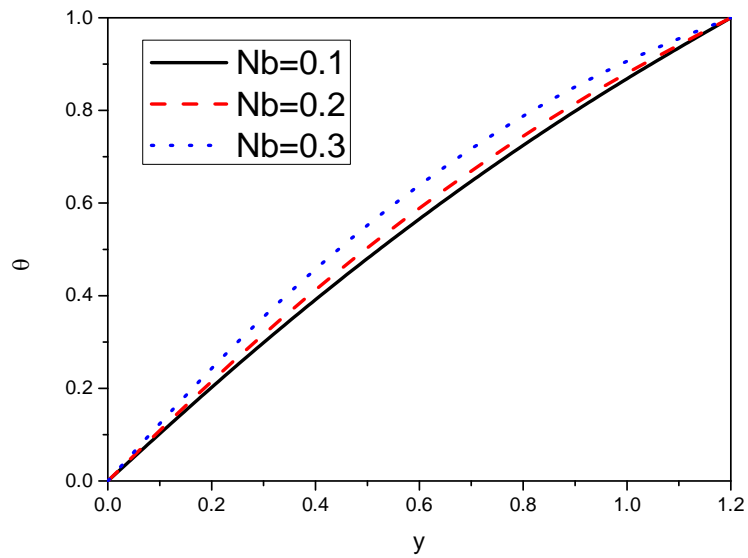


FIGURE 8 Temperature profile for different values of Nb
 When $Nt = 0.5$, $Pr = 1$, and $Rd = 0.9$

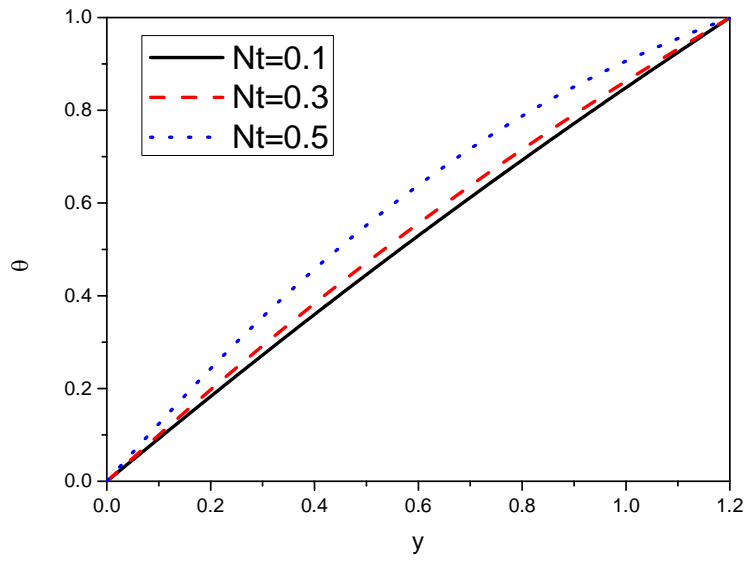


FIGURE 9 Temperature profile for different values of Nt
When $Nb = 0.3$, $Pr = 1$, and $Rd = 0.9$

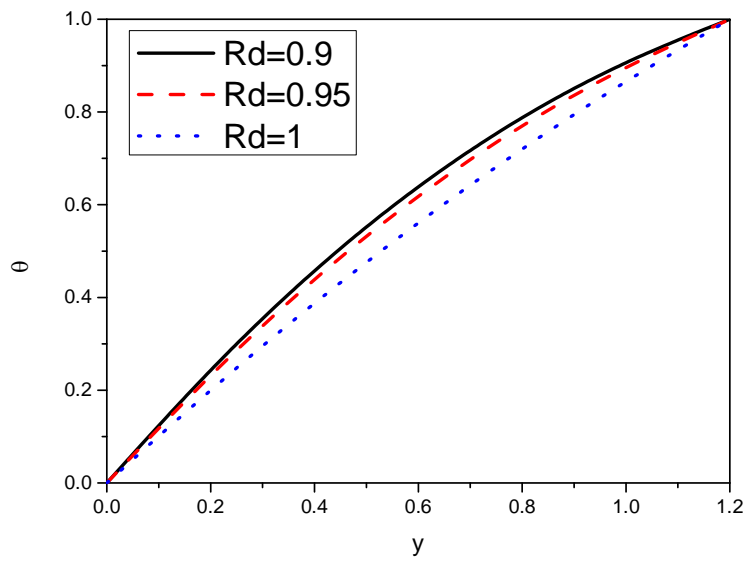


FIGURE 10 Temperature profile for different values of Rd
When $Nb = 0.3$, $Pr = 1$, and $Nt = 0.5$

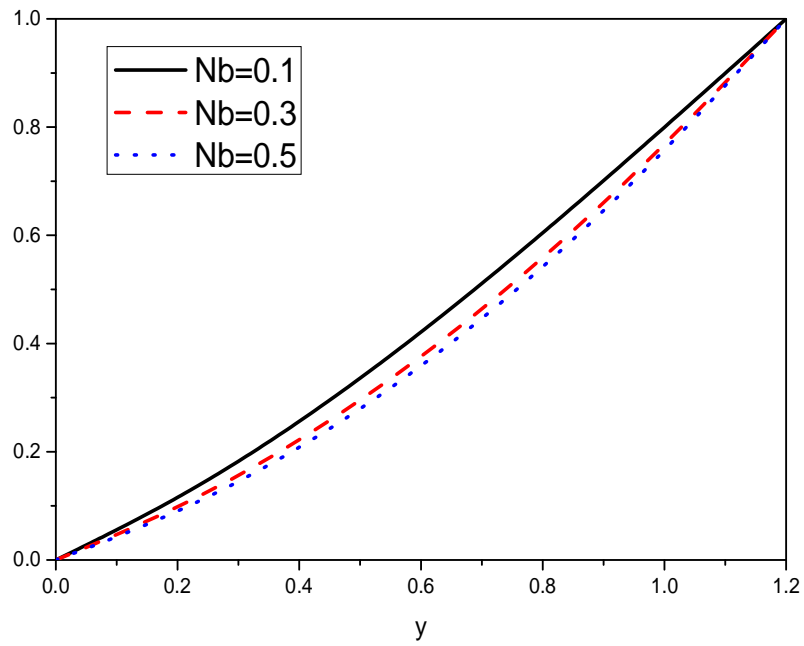


FIGURE 11 Solutal (species) concentration profile for different values of Nb
 When $N_{CT}=0.8$, $Nt=0.1$, $Pr=7.0$, and $Rd=0.1$

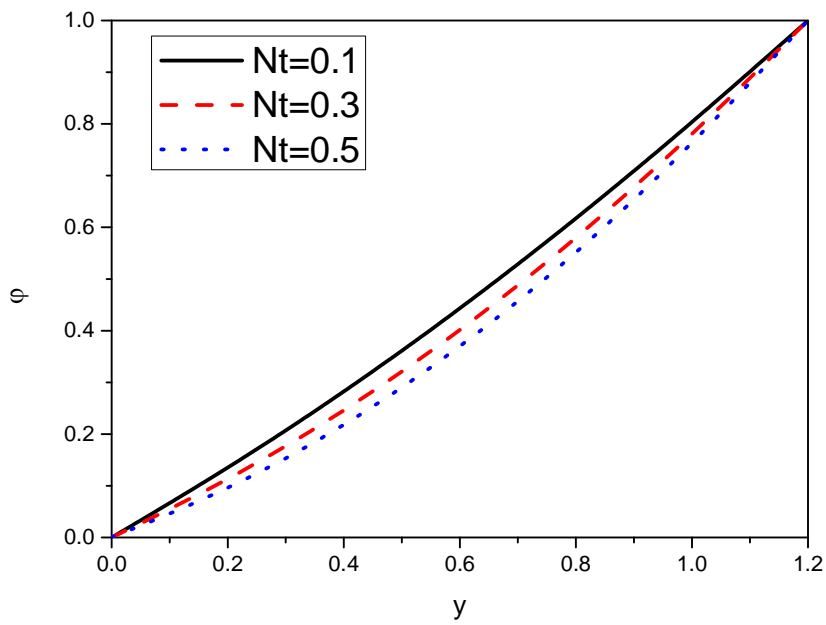


FIGURE 12 Solutal (species) concentration profile for different values of Nt
 When $N_{CT}=0.8$, $Nb=0.1$, $Pr=7.0$, and $Rd=0.1$

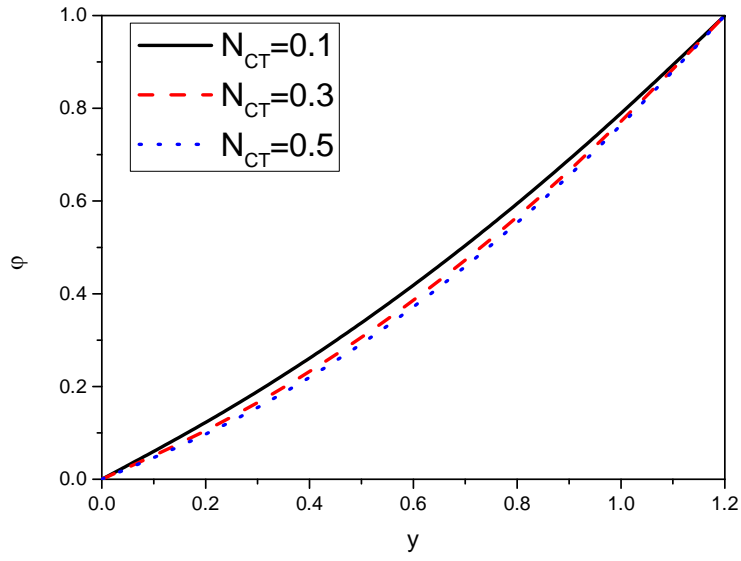


FIGURE 13 Solutal (species) concentration profile for different values of N_{CT}
 When $Nt=0.6$, $Nb=0.1$, $Pr=7.0$, and $Rd=0.1$

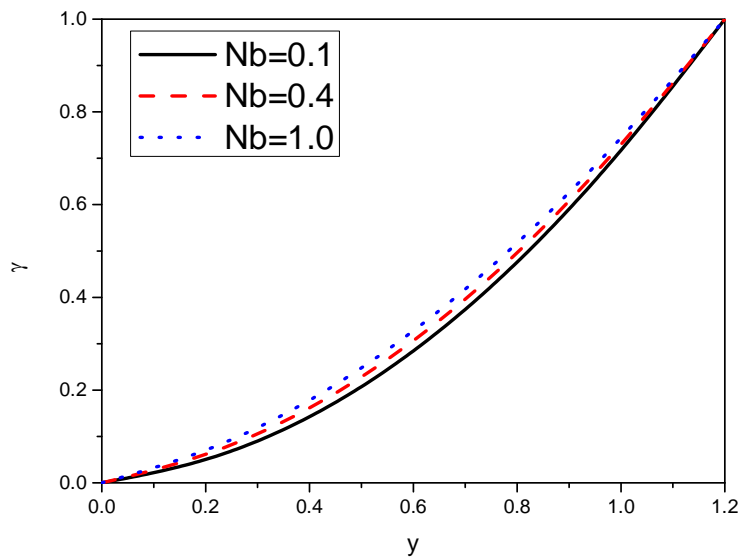


FIGURE 14 Nanoparticle volume fraction profile for different values of Nb
 When $Nt=0.5$, $Pr=7.0$, and $Rd=0.1$

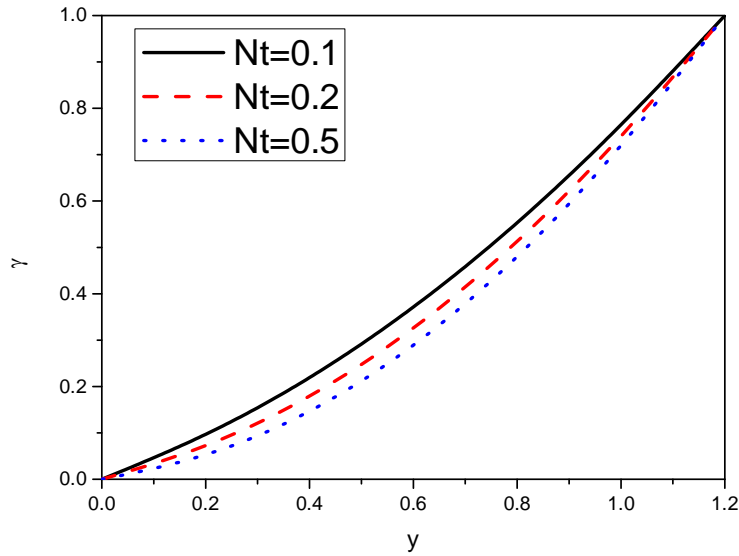


FIGURE 15 Nanoparticle volume fraction profile for different values of Nt
When $Nb = 0.1$, $Pr = 7.0$, and $Rd = 0.1$

5 Conclusion

This research work investigates the double diffusion on peristaltic flow of nanofluid in the presence of porous medium and thermal radiation through nonuniform channel. The results of the present method are in excellent agreement with the HAM [16]. However, it is worth mentioning that the HPSTM finds the solution without any initial guess or auxiliary linear operator and avoids the round-off errors, and it is capable of reducing the volume of the computational work as compared to the HAM while still maintaining the high accuracy of the numerical result and the size reduction amounts to an improvement of the performance of the approach.

The important observations are listed below.

- The present work has potential in biomedical, engineering, and industrial applications.
- The behaviour of relaxation to retardation time on velocity and pressure rise are opposite.
- Opposite behaviours on temperature profile is noted for Nb and Rd .
- Behaviour of Gr_F and Gr_C on pressure rise is too similar, that is, increases for N_{TC} and N_{CT} slightly enhanced the temperature of the wall surface.
- Opposite behaviour of Gr_T and Gr_C on velocity profile and pressure rise profile.
- The behaviour of Gr_T and Gr_C on pressure rise are similar.
- The similar behaviour of Nb , Nt , N_{CT} on solutal (species) concentration profile. Here, solutal concentration profile enhanced with higher values of Nb , Nt , N_{CT} .
- Opposite behaviour of Nt and Nb on nanoparticle volume fraction profile.

Nomenclature

t' time (seconds)

p' pressure in fixed frame (Pa)

h_1' right wall

h_2' left wall

Rd Reynolds number

u', v' velocity components (m/s)

Pr Prandtl number

T' temperature (K)

ϕ' nanoparticle volume fraction

D_B Brownian diffusion coefficient (m²/s)

Gr_F nanoparticle Grashof number

T_m fluid mean temperature (K)

Gr_T thermal Grashof number

F' solutal species concentration

N_{CT} Soret parameter

Nb Brownian motion parameter

Gr_C solutal Grashof number

REFERENCES

1. T.W.Latham, Fluid motion in peristaltic pump, *M.S. Thesis, MIII, Cambridge, MA*(1966).
2. A.H.Shapiro, M.Y.Jaffrin and S.L.Weinberg, Peristaltic pumping with long wavelength at low Reynolds number, *J FluidMech*,17 (1969)799-825.
3. M.Y.Jaffrin and A.H.Shapiro, Peristaltic pumping, *Annu Rev Fluid Mech*,3 (1971) 13-36.
4. B. B. Gupta and V. J. Seshadri, Peristaltic pumping in non-uniform tubes, *Journal of Biomechanics*, 9(1976) 105-109.
5. L. M. Srivastava and V. P. Srivastava, Peristaltic transport of a physio-logical fluid, part I: Flow in non-uniform geometry, *Biorheology*, 20(1983) 153-166.
6. S. K. Asha and G. Sunitha, Peristaltic transport of Eyring-Powell nanofluid in a non-uniform channel, *Jordan J Math Stat*,12(3)(2019) 431-453.
7. S. K. Asha and G. Sunitha, Effect of joule heating and MHD on peristaltic blood flow of Eyring-Powell nanofluid in a non-uniform channel, *J Taibah Univ Sci*,13(1) (2019)155-168.
8. G. Radhakrishnamacharya and V. Radhakrishna Murthy, Heat transfer to peristaltic transport in a non-uniform channel, *Def. Sci. J*, 43 (1993)275-280.
9. S. Akram, M. Zafar and S. Nadeem, Peristaltic transport of a Jeffrey fluid with double-diffusive convection in nanofluids in the presence of inclined magnetic field, *Int J Geom Meth Mod Phys*,15 (2018) 1850181.
10. S. K. Asha and G. Sunitha, Influence of thermal radiation on peristaltic blood flow of a Jeffrey fluid with double diffusion in the presence of gold nanoparticles, *Inform Med Unlocked*,17 (2019) 100272.
11. Shivappa Kotnurkar A and Giddaiah S, Double diffusion on peristaltic flow of nanofluid under the influences of magnetic field, porous medium, and thermal radiation, *Engineering Reports*,2 (2020),e12111.
12. T.Hayat, Quratulain, F.Alsaadi, M Rafiq and B.Ahmad, On effects of thermal radiation and radial magnetic field for peristalsis of sutterby liquid in a curved channel with wall properties, *Chin J Phys*,55 (2017) 2005-2024.
13. Waqas. T. Hassan, S. U. Khan, M. Imran and M. M. Bhatti, Thermally developed Falkner-Skan bioconvection flow of a magnetized nanofluid in the presence of a motile gyrotactic microorganism: Buongiorno's nanofluid model, *Physica Scripta*, 94(11)(2019)115304.

14. Q. Hussain, T. Latif, N. Alvi and S. Asghar, Nonlinear radiative peristaltic flow of hydromagnetic fluid through porous medium, *Results Phys*,9 (2018) 121-134.
15. S.K. Asha and G. Sunitha, Thermal radiation and hall effects on peristaltic blood flow with double diffusion in the presence of nanoparticles, *Case Stud TherEng*,17 (2020) 100560.
16. S. Weerakoon, Application of Sumudu transform to partial differential equations, *International Journal of Mathematical Education in Science and Technology*, 25 (1994) 277–283.
17. Belgacem, F.B.M, Karaballi, A.A, Kalla and L.S, Analytical Investigations of The Sumudu Transform and Applications to Integral Production Equations,*Math. Probl. Engr*, 3 (2003) 103-11.
18. G.K. Watugala, Sumudu Transform - a new integral transform to solve Differential equations and control engineering problems,*Int. J. Math. Educ. Sci. Technol*, 24(1)(1993) 35-43.
19. G.K. Watugala , Sumudu transform – a new imtegral transform to solve differential equations and control engineering problems,*Int. J. Math. Educ .Sci.Technol*,24 (1) (1995) 35-43.
20. H. Eltayeb and A. Kılıçman, A note on the Sumudu transforms and differential equations, *Applied Mathematical Sciences*, 4 (2010) 1089–1098.